LANDSLIDE TSUNAMI AMPLITUDE PREDICTION IN A NUMERICAL WAVE TANK

Stéphan T. Grilli[1], M.ASCE, Sylvia Vogelmann[1], and Philip Watts [2]

Abstract: Tsunami generation by underwater landslides is simulated in a three-dimensional (3D) Numerical Wave Tank (NWT) solving fully nonlinear potential flow equations. The solution is based on a higher-order Boundary Element Method (BEM). New features are added to the NWT to model underwater landslide geometry and motion and specify corresponding boundary conditions in the BEM model. A snake absorbing piston boundary condition is implemented on the onshore and offshore boundaries. Results compare well with recent laboratory experiments. Sensitivity analyses of numerical results to the width and length of the discretized domain are conducted, to determine optimal numerical parameters. The (3D) effect of landslide width on tsunami generated is then estimated. Results show that the 2D approximation is applicable when the ratio of landslide width over length is greater than three.

INTRODUCTION

Tsunamis generated by underwater landslides triggered on the continental slope appear to be one of the major coastal hazards for moderate earthquakes (e.g., Tappin et al. 2001). Such tsunamis, indeed, are only limited in height by the landslide vertical displacement, which may reach several thousand meters (Murty 1979; Watts 1998). Hence, huge coastal tsunamis, offering little time for warning, can be produced (Watts 2000).

Predicting landslide tsunamis requires complex numerical models in which both landslide and bottom geometry must be accuratedly represented. The models must also account for nonlinear interactions between landslide motion and surface wave field. Grilli and Watts (1999) implemented such of a two-dimensional (2D) numerical model, based on a higher-order Boundary Element Method (BEM), i.e., a Numerical Wave Tank (NWT). Reviews of the literature to

[1]Dept. of Ocean Engng., University of Rhode Island, Narragansett, RI 02882, USA. E-mail: grilli@oce.uri.edu.

[2]Applied Fluids Engng., Inc., Mail Box #237, 5710 E. 7th Street, Long Beach, CA 90803, USA. E-mail: phil.watts@appliedfluids.com

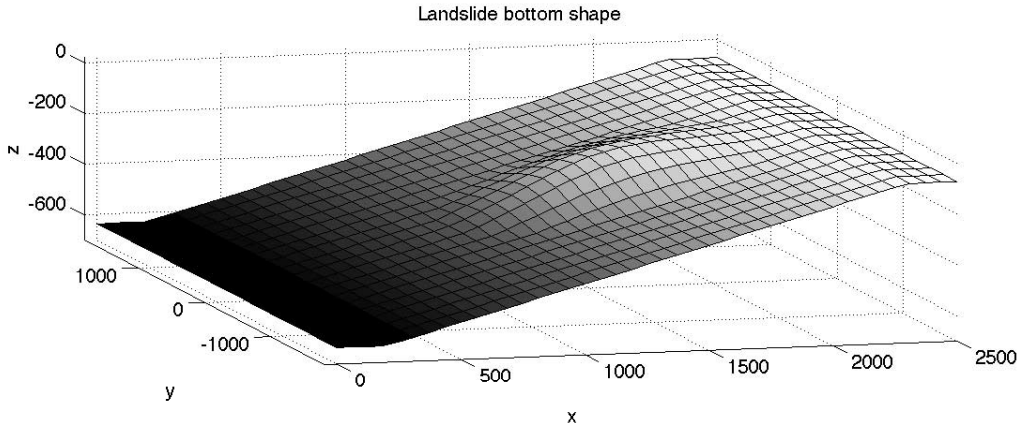

FIG. 1. Example of underwater landslide geometry over a plane 15 degree slope, modeled in the 3D-NWT.

date regarding tsunamis generated by underwater landslides and their numerical modeling can be found in the latter paper and in Watts and Grilli (2001). Here, we describe the current implementation, validation, and simulation of tsunami generation by underwater landslides in the three-dimensional (3D) NWT developed by Grilli et al. (2001). Fully nonlinear potential flow equations are solved in this NWT, based on a higher-order Boundary Element Method and an explicit time stepping scheme. Wave overturning can be modeled if it occurs in the computations. Grilli et al. validated their 3D-NWT for solitary wave shoaling and breaking over slopes, by comparing results both to experiments and to an earlier numerical solution. The agreement was excellent.

In the present work, various improvements were made to the 3D-NWT, to simulate tsunamis caused by underwater landslides. Open boundary conditions were implemented, and validated for solitary wave propagation over constant depth (Grilli and Watts 2001). These conditions extend to 3D the piston-like boundary condition developed by Clément (1996) and Grilli and Horrillo (1997). The landslide shape and kinematics were modeled on a way similar to the Grilli and Watts (1999) 2D model, by assuming a smooth initial shape for the landslide, moving down a planar slope (e.g., Figs. 1 and 2).

NWTs enable many outputs to be obtained with minimal error, and in virtually no setup time (free surface profiles, numerical wave gages, runup, etc...). Here, however, as done in earlier 2D studies, we will represent results of the 3D-NWT by a characteristic wave amplitude calculated above the initial landslide position, at the location of maximum landslide thickness (defined at horizontal location $(x_g, 0)$; Fig. 3). Our characteristic wave amplitude is thus an implicit

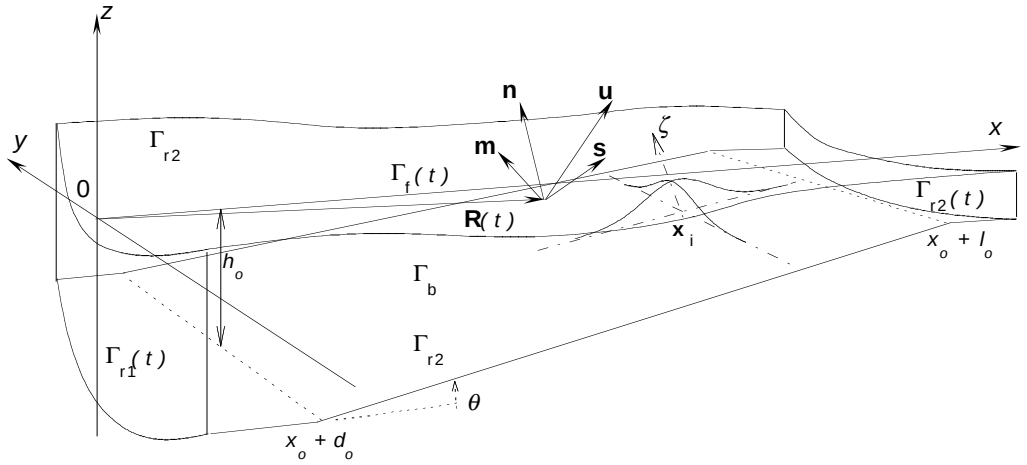

FIG. 2. Sketch of 3D-NWT used for landslide tsunami modeling.

function of the underwater landslide shape and motion input parameters.

THE NUMERICAL WAVETANK

Governing equations and boundary conditions

Fully nonlinear potential free surface flow equations are solved in the 3D-NWT. These are summarized below. The velocity potential $\phi(\boldsymbol{x},t)$ describes inviscid irrotational 3D flows in Cartesian coordinates $\boldsymbol{x}=(x,y,z)$, with z the vertical upward direction (and $z=0$ at the undisturbed free surface; Fig. 2). The velocity is defined by, $\boldsymbol{u}=\boldsymbol{\nabla}\phi=(u,v,w)$.

Mass conservation in the fluid domain $\Omega(t)$, with boundary $\Gamma(t)$, is a Laplace's equation for the potential,

$$\nabla^2\phi=0 \qquad\qquad \text{in } \Omega(t) \tag{1}$$

Green's second identity transforms Eq. (1) into the Boundary Integral Equation (BIE),

$$\alpha_l\,\phi_l=\int_\Gamma\left\{\frac{\partial\phi}{\partial n}(\boldsymbol{x})\,G(\boldsymbol{x},\boldsymbol{x}_l)-\phi(\boldsymbol{x})\,\frac{\partial G}{\partial n}(\boldsymbol{x},\boldsymbol{x}_l)\right\}\mathrm{d}\Gamma \tag{2}$$

in which $\alpha_l=\alpha(\boldsymbol{x}_l)=\theta_l/(4\pi)$, with θ_l the exterior solid angle made by the boundary at point $\boldsymbol{x}_l$ (i.e., 2π for a smooth boundary), with the 3D free space Green's functions defined as,

$$G=\frac{1}{4\pi\,r}\quad\text{with}\quad\frac{\partial G}{\partial n}=-\frac{1}{4\pi}\,\frac{\boldsymbol{r}\cdot\boldsymbol{n}}{r^3} \tag{3}$$

where $\boldsymbol{r}=\boldsymbol{x}-\boldsymbol{x}_l$, $r=\mid\boldsymbol{r}\mid$, $\boldsymbol{x}$ and $\boldsymbol{x}_l=(x_l,y_l,z_l)$ are points on boundary Γ, and $\boldsymbol{n}$ is the outward unit vector normal to the boundary at point $\boldsymbol{x}$.

The boundary is divided into various sections, with different boundary conditions (Fig. 2). On the free surface $\Gamma_f(t)$, ϕ satisfies the nonlinear kinematic and dynamic boundary conditions,

$$\frac{D\,\boldsymbol{R}}{D\,t} = \boldsymbol{u} = \boldsymbol{\nabla}\phi \qquad \text{on } \Gamma_f(t) \tag{4}$$

$$\frac{D\,\phi}{D\,t} = -gz + \frac{1}{2}\,\boldsymbol{\nabla}\phi\cdot\boldsymbol{\nabla}\phi - \frac{p_a}{\rho_w} \qquad \text{on } \Gamma_f(t) \tag{5}$$

respectively, with $\boldsymbol{R}$ the position vector of a free surface fluid particle, g the acceleration due to gravity, p_a the atmospheric pressure, ρ_w the fluid density, and D/Dt the material derivative.

Various methods can be used for wave generation in the NWT. Here, tsunamis are generated on the free surface due to a landslide motion $\boldsymbol{x}_\ell(t)$ specified on the bottom boundary Γ_b (Figs. 1 and 2). We have, for landslide geometry and kinematics,

$$\overline{\boldsymbol{x}} = \boldsymbol{x}_\ell \;\;;\;\; \overline{\frac{\partial\phi}{\partial n}} = \boldsymbol{u}_\ell\cdot\boldsymbol{n} = \frac{\mathrm{d}\,\boldsymbol{x}_\ell}{\mathrm{d}\,t}\cdot\boldsymbol{n} \qquad \text{on } \Gamma_b(t) \tag{6}$$

where overlines denote specified values, and the time derivative follows the landslide motion. See below for details.

Along stationary parts of the boundary, such as part of the bottom and some lateral parts of Γ_{r2}, a no-flow condition is prescribed as,

$$\overline{\frac{\partial\phi}{\partial n}} = 0 \qquad \text{on } (\Gamma_{r2}),\ (\Gamma_b). \tag{7}$$

Assuming the landslide motion is in the negative x direction, actively absorbing boundary conditions are specified at one or both extremities of the NWT in the x direction, initially at $x = x_o$ and $x_o + L_0 + l_1$ (Figs. 2 and 3). These are modeled as pressure sensitive "snake" absorbing piston wavemakers. The piston normal velocity is specified as,

$$\overline{\frac{\partial\phi}{\partial n}} = u_{ap}(\sigma,t) \qquad \text{on } \Gamma_{r2}(t), \text{ with,} \tag{8}$$

$$u_{ap}(\sigma,t) = \frac{1}{\rho_w h_0\sqrt{g h_0}}\int_{-h_0}^{\eta_{ap}(\sigma,t)} p_D(\sigma,z,t)\,\mathrm{d}z \tag{9}$$

calculated at curvilinear abscissa σ, horizontally measured along the piston boundary, where η_{ap} is the surface elevation at the piston and $p_D = -\rho_w\{\frac{\partial\phi}{\partial t} + \frac{1}{2}\nabla\phi\cdot\nabla\phi\}$ denotes the dynamic pressure. The integral in Eq. (9) represents the horizontal hydrodynamic force $F_D(\sigma,t)$ acting on the piston at time t, as a function of σ.

For well-posed problems, we have, $\Gamma \equiv \Gamma_f \cup \Gamma_b \cup \Gamma_{r1} \cup \Gamma_{r2}$.

Time integration

Second-order explicit Taylor series expansions are used to express both the new position $\boldsymbol{R}(t+\Delta t)$ and the potential $\phi(\boldsymbol{R}(t+\Delta t))$ on the free surface, in a mixed Eulerian-Lagrangian formulation. The adaptive time step Δt in the Taylor series is calculated at each time, from the minimum distance between nodes on the free surface, ΔR_o, and a constant mesh Courant number $\mathcal{C}_o = \Delta t\sqrt{gh_o}/\Delta R_o \simeq 0.5$ (see Grilli et al. 2001 for details).

First-order coefficients in the Taylor series are given by Eqs. (4) and (5), which requires calculating $(\phi,\ \frac{\partial \phi}{\partial n})$ on the free surface. This is done by solving Eq. (2) at time t, with boundary conditions (6) to (9). Second-order coefficients are obtained from the material derivative of Eqs. (4) and (5), which requires calculating $(\frac{\partial \phi}{\partial t},\ \frac{\partial^2 \phi}{\partial t \partial n})$ at time t. This is done by solving a BIE similar to Eq. (2) for the $\frac{\partial \phi}{\partial t}$ field. The free surface boundary condition for this second BIE is obtained from Bernoulli Eq. (4), after solution of the first BIE for ϕ.

BEM discretization

The spatial discretization in the NWT follows that of the Grilli et al. (2001) model. All details can be found in the latter reference.

In short, the BIEs for ϕ and $\frac{\partial \phi}{\partial t}$ are solved by a BEM. The boundary is discretized into collocation nodes and 2D cubic sliding boundary elements, based on polynomial shape functions. These are expressed over 4 by 4 node reference elements, of which only one 4-node quadrilateral is used as the actual boundary element. Curvilinear changes of variables are used for expressing boundary integrals over reference elements and deriving discretized equations. Discretized boundary integrals, both regular and singular, are calculated for each collocation node by numerical Gauss quadrature (special methods are used to regularize singular integrals, based on polar coordinate transformations in the reference element). Double and triple nodes and edges are used at intersecting parts of the boundary. The BEM algebraic system of equations is solved in the present applications using a direct elimination method.

Tangential derivatives, e.g., needed in the Taylor series, are calculated on the boundary in a local curvilinear coordinate system $(\boldsymbol{s}, \boldsymbol{m}, \boldsymbol{n})$ defined at each boundary node (Fig. 2), with $\boldsymbol{s} = \boldsymbol{x}_s$, $\boldsymbol{m} = \boldsymbol{x}_m$, and $\boldsymbol{n} = \boldsymbol{s} \times \boldsymbol{m}$ (subscripts indicate partial derivatives). Derivatives of the geometry and field variables in tangential directions $\boldsymbol{s}$ and $\boldsymbol{m}$ are computed, by defining, around each node, a local 5 node by 5 node, 4th-order, sliding element.

Landslide geometry and discretization

In the Grilli and Watts (1999) model, semi-ellipses were used to represent the geometry of 2D vertical landslide cross-sections, which were then moved downslope according to a specified landslide kinematics. Sharp corners occurred at the intersections between the landslide and the planar slope, causing singularities in the BEM solution. This required refining the discretization near corners.

Here, 3D underwater landslides are represented by a fully submerged smooth sediment mound of density ρ_ℓ, sitting over a plane slope of angle θ (Figs. 1 to

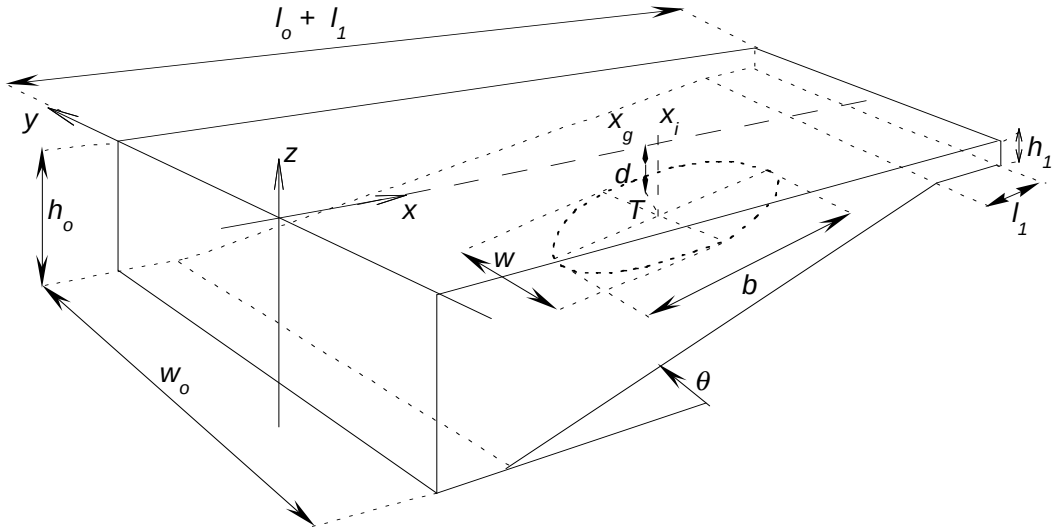

FIG. 3. Definition of 3D-NWT and landslide geometrical parameters.

3). The landslide has maximum thickness T (measured perpendicularly to the slope). The middle of the landslide surface is located in depth d, at a distance x_g along the x-axis. The geometry is represented by $T\,\mathrm{sech}^2(k\,r_\ell)$ curves, in polar coordinates (r_ℓ, φ_ℓ) defined within the slope and centered on the landslide axis intersection with the slope, at point $\boldsymbol{x}_i = (x_i, y_i, z_i)$. These curves are truncated at points where they reach an elevation $\varepsilon\,T$ above the slope. This geometric model provides for a smoother bottom geometry than ellipses. The landslide, in fact, is simply treated as a "wave" of bottom elevation moving downslope. The landslide footprint on the slope is defined as an ellipse of major axis b (in the x direction) and minor axis w (in the y direction) (Fig. 3). These dimensions are expressed as functions of specified characteristic dimensions (B, W) which, with T, define the landslide volume. Coefficients $k(\varepsilon, \varphi_l, b, w)$ in the definition of landslide geometry are defined based on these parameters. For the sake of simplicity and comparison with other work, it is assumed that the landslide volume is identical to that of the semi-ellipsoid defined by (B, W, T).

In the NWT, the maximum number of nodes/elements that can be used in the domain discretization is limited by the available computer memory. To select an optimal size and resolution of the discretization, a tsunami characteristic wave length was defined by Grilli and Watts (1999), based on theoretical scaling considerations, as,

$$\lambda_o \simeq t_o\sqrt{g\,d} \tag{10}$$

where t_o is a characteristic time defined below. In all cases, the domain length (x direction) was selected close to that value, and at least $M_x = 20$ elements were used to discretize one theoretical wavelength.

Landslide motion

We follow the wavemaker formalism developed by Watts (1998). Dimensional analysis shows that, within a family of similar landslide geometry, landslide motion and tsunami characteristics are functions of the five nondimensional independent parameters : $\gamma = \rho_\ell/\rho_w$, θ, d/b, T/b, and w/b. Accordingly, one can derive an approximate equation describing the center of mass motion $S(t)$ (parallel to the planar slope in the negative x direction), for rigid underwater landslides, starting at rest at $t = 0$ (see Watts and Grilli (2001) for details). We find,

$$S(t) = S_o \ln\left(\cosh\frac{t}{t_o}\right) \tag{11}$$

with,

$$S_o = \frac{u_t^2}{a_o} \;\; ; \;\; t_o = \frac{u_t}{a_o} \tag{12}$$

where S_o and t_o are characteristic length and time of motion, respectively, and a_o and u_t denote landslide initial acceleration and terminal velocity, respectively, given by,

$$a_o = g\,\frac{\gamma - 1}{\gamma + C_m}\,\sin\theta \tag{13}$$

where C_m is an approximate added mass coefficient, and,

$$u_t = \sqrt{gB}\sqrt{\frac{\pi(\gamma-1)}{2\,C_d}\,\sin\theta} \tag{14}$$

where C_d is an approximate drag coefficient. Watts (1998) and Watts (2000) found added mass and drag coefficients to be of $\mathcal{O}(1)$ for 2D and quasi-2D landslides (for which $W \gg B$). [Note that Coulomb friction was neglected in this analysis.]

APPLICATIONS

To compare results with an earlier 2D model and with recent laboratory experiments, a quasi-2D landslide case was run by Grilli and Watts (2001), for which $W \gg B$ and, hence, there is no lateral (y) variation in landslide geometry. Therefore, the 3D-NWT problem becomes equivalent to a 2D slice along a uniform landslide, similar to cases solved in the 2D model by Grilli and Watts (1999). The agreement with 2D results and with the experiments was found to be quite good for both the characteristic tsunami amplitude and the time evolution of free surface elevation at numerical gages.

Here, we consider a landslide of similar parameters as in this quasi-2D case, i.e. : slope angle $\theta = 15°$, rigid landslide with average density $\rho_\ell = 1,900$ kg/m^3 (and thus $\gamma = 1.845$ for $\rho_w = 1,030$ kg/m^3), length $B = 1,000$ m (and thus $b = 1,299$ m for $\varepsilon = 0.5$) and maximum thickness $T = 50$ m, and initial submergence $d = 260$ m. Now, however, there is a lateral y variation in landslide geometry and a full 3D landslide geometry is modeled as discussed above (Fig. 1). The

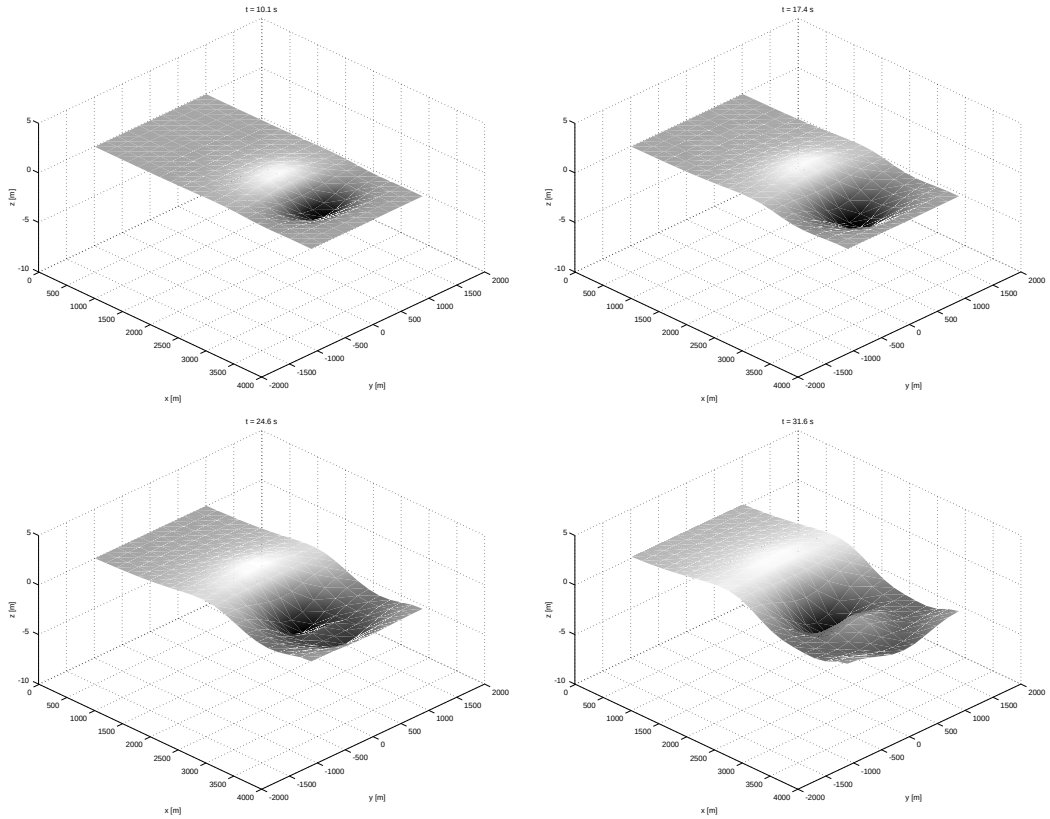

FIG. 4. Surface elevation at different times for a 3D landslide tsunami simulation with : $\theta = 15$ deg., $B = 1000$ m, $W = 1000$ m, $T = 50$ m, $d = 260$ m, $L_0 = l_0 + l_1 = \lambda_0 = 3888$ m, $w_0 = 2000$ m, $d_0 = 400$ m, $h_0 = 1,031$ m, $l_1 = 300$ m, $h_1 = 70$ m.

computational domain is such as sketched in Fig. 3. The offshore boundary is represented by an absorbing piston and all other lateral boundaries are assumed impermeable. The shallow shelf at the onshore extremity has depth $h_1 = 70$ m and length $l_1 = 300$ m. The constant depth offshore region has a length $d_o = 400$ m (with $x_o = 0$), and its depth $h_o = h_1 + L_0 \tan\theta$ depends on the selected domain length. The landslide kinematics is computed based on Eqs. (11) to (14). The hydrodynamic coefficients are set to the standard values $C_m = 1$, $C_d = 1$. With this data, the landslide kinematics is defined by : $S_o = 4,469$ m, $u_t = 58.1$ m/s, $a_o = 0.754$ m/s^2, and $t_o = 77.0$ s, and, based on this, we find an approximate tsunami wavelength $\lambda_o = 3,888$ m.

To assess the effects of discretization and boundary conditions on 3D-NWT results, we study the sensitivity of tsunami characteristic amplitude η_c to the length $L_0 = L_0 + l_1$ and width w_0 of the computational domain. Sensitivity of results to slope angle θ, landslide length B, thickness T, initial submergence d, and density, was studied by Watts and Grilli (2001), using the 2D model by Grilli and Watts (1999). Emprical relationships were derived, through curve fitting of numerical results, between the dimensionless tsunami characteristic amplitude

η_c/S_o and dimensionless parameters : $\sin\theta, B/d, T/B$, and γ. These relationships are essentially applicable to 3D results. Here, to assess 3D effects on tsunami generation, we study the sensitivity of η_c to the dimensionless landslide width W/B.

Only rigid landslides are simulated in this study. Watts and Grilli (2001) investigated the influence of landslide deformation, in the form of a linear landslide extension in the downslope direction during failure. They found that the impact of this deformation on the characteristic amplitude was negligible as a first approximation.

For a domain length $L_0 = \lambda_o$, with $h_o = 1031$ m, $W = B$, and $w_0 = 2W$, we specify 20 BEM elements in the x direction, of initial length $\Delta x_o = 194.4$ m, 10 elements in the width y direction, of length $\Delta y_o = 200$ m, and 4 elements over depth. With this data, the initial time step is set to $\Delta t_o = 0.45\,\Delta x_o/\sqrt{g\,h_o} = 0.87$ s. Fig. 4 shows free surface elevations computed in this case, at various times $t = 0$ to 31.6 s. We see the appearance of an initial dipole-like surface elevation, with a wave of depression forming above the landslide initial location and a wave of elevation propagating offshore of the landslide. Later on ($t > 21$ s), a smaller wave of elevation is seen to also propagate onshore, which would eventually induce coastal flooding and runup. For this case, the maximum error on mass conservation was 0.82% of the landslide volume.

We maintain the same density of discretization and initial time step for other cases studied in the following sensitivity analysis, using different domain length and width, and landslide width.

Effect of domain length

For simplicity, cases with no variation in the y-direction ($W = \infty$), are modeled. The domain width is set to $w_0 = B$ for all calculations. The total domain length L_0 is set to multiples of the theoretical wavelength λ_o (0.6 to 3). For fully developed quasi-2D tsunami generation we find $\eta_{c2D} \simeq 6.0$ m. For $L_0 > \lambda_o$, little change is observed in η_{c2D}. Hence, this value is used for domain length in the following.

Effect of domain width

Here, we verify at which distance, $y = \pm w_0/2$, the impermeable lateral boundaries have to be located to avoid perturbing the tsunami generation process, i.e., changing η_c through reflection. To do so, landslides of different widths $W = B$, $2B$ and $3B$ are modeled and, for each width, calculations are performed using different domain widths $w_0 = W$ to $3 - 6W$. Results show that, for a ratio $w_0/W \geq 2$, η_c only varies very slightly. Hence, this ratio is used in the following.

Effect of landslide width

Landslides of various widths $W = B/2$ to $3B$ are modeled and the resulting η_c compared. Results show an increase in η_c with increasing landslide aspect ratio W/B. The large initial increase with W/B, however, becomes slower for $W/B > 2$, where the amplitude eventually approaches its 2D value asymptotically. For the current results, we find $\eta_c \simeq \eta_{c2D} - 2.36(W/B)^{-1.35}$ (with $R^2 = 0.95$).

CONCLUSIONS

Landslide tsunami generation mechanisms were explored in a 3D-NWT solving fully nonlinear potential flow equations, using a higher-order BEM. Accurate modeling of underwater landslide geometry and motion, and snake absorbing piston boundaries and their efficiency, were illustrated in the applications. Experimental validation of results was reported elsewhere for a quasi-2D landslide.

For one realistic set of landslide parameter values, we conclude that the characteristic tsunami amplitude η_c is not significantly affected when the width of the computational domain $w_0 \geq 2W$ and the length of the computational domain $L_0 \geq \lambda_o$, respectively. We also find that the 3D η_c converges towards the 2D value for $W \geq 2B$. The latter result is of importance as 2D analyses (such as described in Grilli and Watts (1999) and Watts and Grilli (2001)) are much easier and quicker to carry out than 3D studies, particularly in a realtime forecasting situation. It is therefore of interest to assess whether 2D conditions can be assumed in a given case and the corresponding simplified model applied.

REFERENCES

Clément, A. (1996). "Coupling of two absorbing boundary conditions for 2d time-domain simulations of free surface gravity waves." *J. Comp. Phys.*, 26, 139–151.

Grilli, S., Guyenne, P., and Dias, F. (2001). "A fully nonlinear model for three-dimensional overturning waves over arbitrary bottom." *Intl. J. Numer. Methods in Fluids*, 35(7), 829–867.

Grilli, S. and Horrillo, J. (1997). "Numerical generation and absorption of fully nonlinear periodic waves." *J. Engng. Mech.*, 123(10), 1060–1069.

Grilli, S. and Watts, P. (1999). "Modeling of waves generated by a moving submerged body. Application to underwater landslides." *Engng. Analysis with Boundary Elts.*, 23, 645–656.

Grilli, S. and Watts, P. (2001). "Modeling of tsunami generation by an underwater landslide in a 3D-NWT." *Proc. 11th Offshore and Polar Engng. Conf. (ISOPE01, Stavanger, Norway)*, Vol. 3. 132–139.

Murty, T. (1979). "Submarine slide-generated water waves in kitimat inlet, british columbia." *J. Geophys. Res.*, 84(C12), 7777–7779.

Tappin, D., Watts, P., McMurtry, G., Lafoy, Y., and Matsumoto, T. (2001). "The Sissano, Papua New Guinea tsunami of July 1998 – offshore evidence on the source mechanism." *Marine Geology*, 175, 1–23.

Watts, P. (1998). "Wavemaker curves for tsunamis generated bu underwater landslides." *J. Waterway, Port, Coastal, and Ocean Engng.*, 124(3), 127–137.

Watts, P. (2000). "Tsunami features of solid block underwater landslides." *J. Waterway, Port, Coastal, and Ocean Engng.*, 126(3), 144–152.

Watts, P. and Grilli, S. (2001). "Tsunami generation by submarine mass failure. Part I : Wavemaker models." *To be submitted to J. Waterway, Port, Coastal, and Ocean Engng.*